QUEST FOR HIGH GRADIENTS

D. Proch
Deutsches Elektronen-Synchrotron DESY, Hamburg, Germany

Abstract
In this chapter the method of reaching high accelerating gradients in superconducting cavities is presented. In the first part fundamentals of cavity design and measurement techniques are described. In the main part field limitation by multipacting, quench and field emission are discussed. Finally the state of the art and recent measurements with single and multicell structures are outlined.

1. INTRODUCTION

There is an increasing number of accelerator projects with superconducting cavities as accelerating structures: storage rings (CERN [1], DESY [2], KEK [3], see Fig. 1), linacs for electrons or positrons (Frascati [4], CEBAF [5], HEPL [6], Darmstadt [7]), linacs for heavy ions (Argonne [8], Legnaro [9], Jaeri [10]), development programmes for high current application (Cornell [11], KEK [12]) and for a superconducting linear collider (TESLA [13]). The advantage of superconducting over normal conducting cavities is that accelerating gradients can be established with less AC power (including the cryogenic plant) and that higher gradients are possible for continuos wave operation. Another advantage of the low power demand is that the cavity geometry does not need to be strictly optimised for minimum power demand. Therefore a shape of the cavity can be chosen which produces less beam-cavity interaction at frequencies higher than the accelerating mode (so-called higher order modes, HOM). Operating systems work at gradients far below the theoretical limit (at less than 20 %) whereas the best values of single-cell measurements come near to this limit. In this chapter I will describe the quest for high gradients by following the historical development of this research area. Finally the state of the art is presented. I will not describe fundamentals of superconductivity (see Schmüser, this course) and basics of RF superconductivity (see Weingarten, this course). I will also concentrate on solid niobium as the cavity material and on those structures which have a phase velocity near, or equal to, the speed of light.

2. SOME CAVITY PROPERTIES

Figure 2 shows the typical shape of a superconducting accelerating structure. The rounded shape is chosen to suppress multipacting (see next sections). The electromagnetic fields inside the cavity are determined by the conditions of Maxwell's equation. For a simple cavity shape (pill box, cylinder) the analytic solution is given in standard text books (for example in [14]). More complex structures can be analysed by finite element programmes, for example URMEL [15] or in 3D by MAFIA [16]). The electric field lines inside the resonator are closed by surface currents in the uppermost metal boundary. The ratio of the accelerating electric field on the axis, the surface current in the metal and the magnetic field at the surface is determined by the cavity shape (and not by the conductivity!). In Fig. 3 typical numbers for the maximum surface electric field (at the iris) and the maximum magnetic field (at the equator) are given for an accelerating field of 1 MV/m. These numbers can be optimised by appropriate shaping of the cavity. The RF loss is proportional to the square of the surface current and inverse proportional to the conductivity. In case of a normal conducting cavity the favourite material is Cu and its conductivity is given. Therefore careful shaping of the cavity is needed to reduce the RF losses.

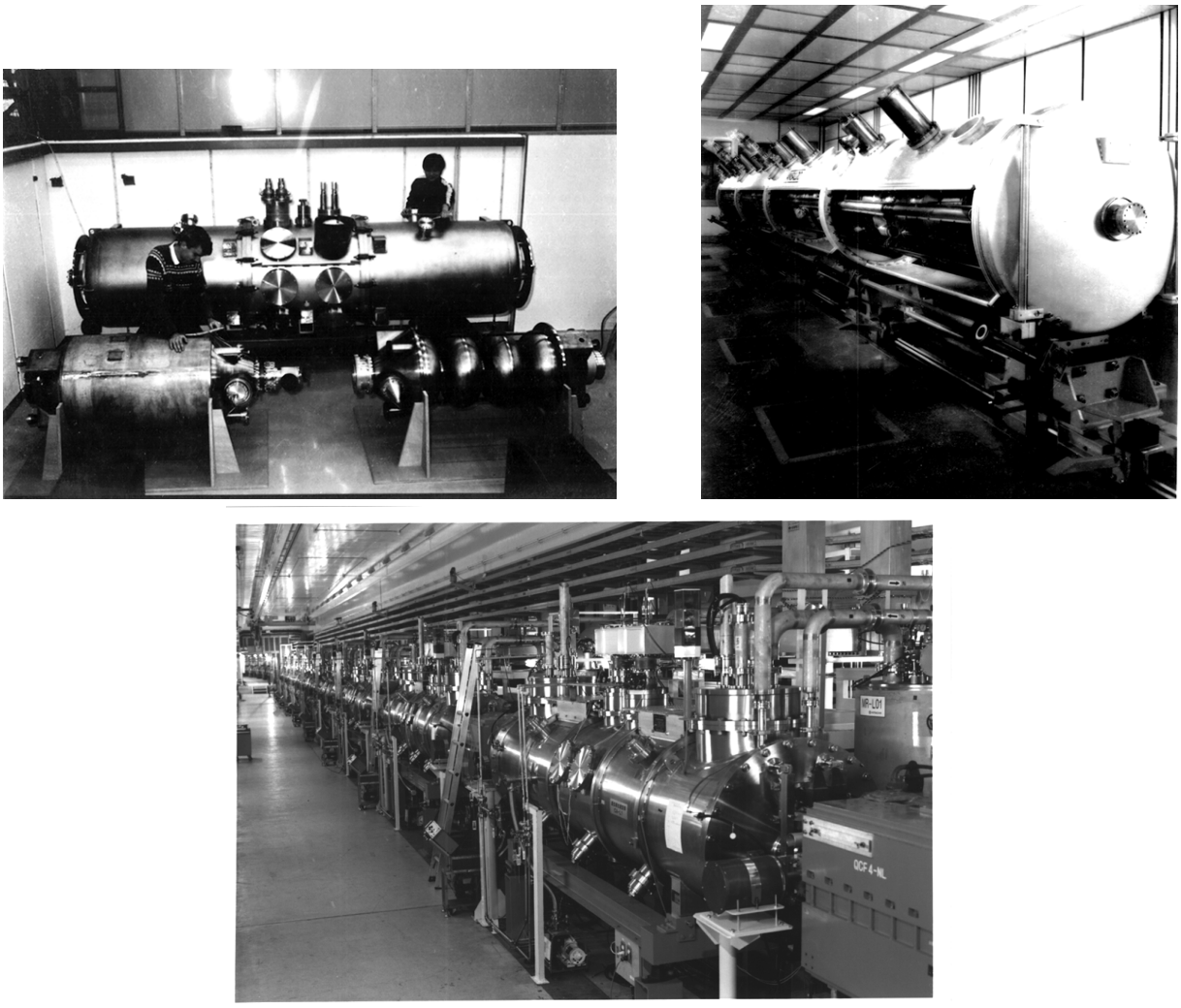

Fig. 1 Examples of superconducting cavity installations. Top left: 500-MHz DESY module with two 4-cell cavities per cryostat, top right: 356-MHz CERN module with four 4-cell cavities per cryostat, bottom: 500-MHz installation at KEK in the TRISTAN tunnel.

Fig. 2 Nine-cell 1.3-GHz cavities for TESLA. The rounded shape of a typical superconducting cavity design is chosen to suppress multipacting.

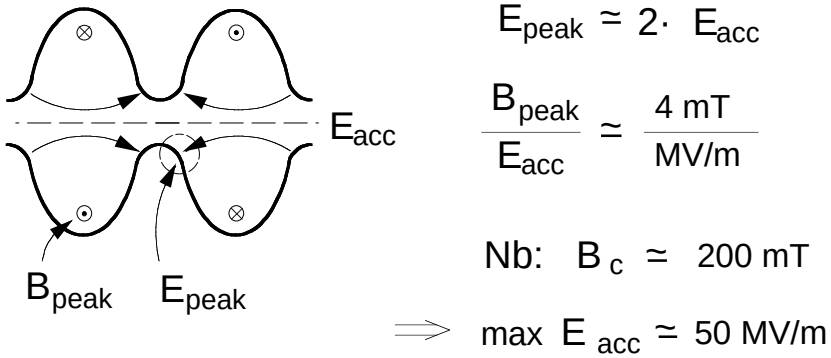

Fig. 3 Cross section of a typical superconducting cavity design. The number for maximum surface electric and magnetic field is given for 1 MV/m accelerating gradient.

For a superconducting cavity the resistivity is enhanced by several orders of magnitude as compared to Cu and is very small (but not zero as for dc current, see Weingarten's chapter). Therefore the shape of a superconducting cavity is optimised for other properties: low excitation of higher frequencies by the beam, low surface magnetic field to enlarge the limit by superconducting- to normal-conducting phase transition, low surface electric field to suppress field emission or appropriate shape to avoid multipacting.

The efficiency of a cavity to produce an accelerating field at a given RF power is defined by the shunt impedance R. This is equivalent to Ohm's law where the resistance is the proportionality factor between the square of the voltage and the loss. Therefore Eq. (1) is called the "Ohm's law for the accelerator":

$$U^2 = R \cdot P \tag{1}$$

where:

U is the accelerating voltage per cavity,

R is the shunt impedance per cavity,

P is the RF power loss per cavity.

At a given power loss P the accelerating voltage can be enlarged by better shaping of the cavity and by using lower-loss wall material. Therefore it is plausible that the shunt impedance can be divided into two factors: R/Q which only depends on the cavity shape and Q which mainly depends on the conductivity of the cavity wall.

$$R = \frac{R}{Q} \cdot Q \tag{2}$$

where:

R/Q is the "cavity shape factor",

Q is the quality factor of the cavity resonator.

Thus Eq. (1) becomes

$$U^2 = \frac{R}{Q} \cdot Q \cdot P \tag{3}$$

The R/Q value can be calculated by several cavity codes or can be measured in comparison with a simple cavity which can be evaluated analytically. Superconducting cavities have a

typical value of R/Q = 100 Ω per cell. As mentioned above, with normal conducting cavities the shunt impedance and thus the R/Q value must be optimised to reduce the RF power. Here typical values of R/Q are around 200 Ω per cell.

The quality factor Q is proportional to the ratio of the stored energy and the power loss

$$Q = \omega \cdot \frac{W}{P} \tag{4}$$

where:

$\omega = 2\pi f$, angular frequency,

W is the stored energy,

P is the RF power loss.

Typical values for Q are 40000 for copper cavities at 500 MHz and 10^{10} for niobium cavities at 1.3 GHz, 1.8 K. With these numbers, one can easily calculate (one cell has a length of 0.5 wavelength) that the RF power loss per metre at 1 MV/m is 37.5 kW for normal conducting and 0.1 W for superconducting cavities. As a rule of thumb the AC power demand of a refrigerator is 1 kW for 1 W cooling power at 1.8 K. Therefore the total power demand for a superconducting cavity is 100 W at this gradient.

2.1 How to measure the accelerating gradient of a superconducting cavity

The accelerating gradient can be measured according to Eq. (3) by knowledge of the geometric factor R/Q and measurement of the quality factor Q and the RF power loss P. The R/Q value can be obtained from programmes like URMEL [15], the power loss P is determined by microwave measurements of the cavity absorbed power. The quality factor Q can be measured by the bandwidth of the resonator according to Eq. (5).

$$Q = \frac{f}{\Delta f} \tag{5}$$

where:

Q is the quality factor,

f is the resonant frequency,

Δf is the bandwidth (full width, half power).

The resonant bandwidth of a superconducting cavity is very small. At a frequency of 1.3 GHz and quality factor of 10^{10}, the bandwidth is just 0.13 Hz and in order to measure the bandwidth, the generator has to be more stable than this. On the other hand the superconducting resonator will vibrate due to noise coming from the cryogenics or the surrounding environment. Therefore the resonance curve itself will move and a fixed, highly-stable oscillator will be unable to excite the resonance. This is why the generator has to be stabilised by the cavity itself (another way is to close a self-excited loop of an amplifier and cavity circuit). Figure 4 shows a resonance curve and the change of the phase of the cavity field when passing through the resonance. This phase information can be used to lock the generator frequency on the centre of the resonance curve. Figure 5 shows the principal microwave circuit of such a stabilisation technique. The phase difference of the forward RF power and the cavity field is measured. The variable phase shifter is adjusted in such a way that the signal is zero at the centre of the resonance curve. Above (below) this frequency, the phase difference is positive (negative). This phase difference signal is converted to an error voltage and finally controls the generator frequency via a frequency tuning circuit.

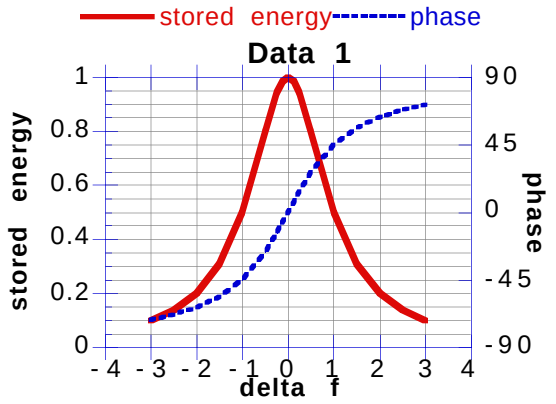

Fig. 4 Amplitude and phase response of a resonator.

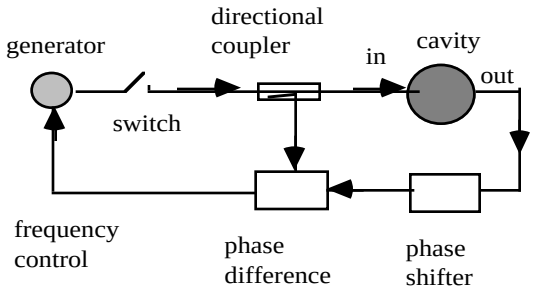

Fig. 5 Principal circuit of a frequency stabilisation system. The phase response of the resonator is used to stabilise the generator to the centre frequency of the resonator.

The quality factor can be determined by measuring the bandwidth according to Eq. (5). But at high Q values this is an inconvenient method. Here it is easier to measure the decay time of the cavity field after switching off the resonator.

$$U(t) = U_0 e^{-\frac{t}{\tau}} \tag{6}$$

where:

$U(t)$ is the cavity field after switching off the generator,

t is the time since switching off the resonator,

U_0 is the cavity field at equilibrium condition,

τ is the time constant of the exponential decay of the cavity field.

The quality factor Q is given by:

$$Q = \omega \cdot \frac{\tau}{2} \tag{7}$$

In Eq. (7) the time constant is $\tau/2$ because the quality factor Q is related to the stored energy (which is proportional to the square of the cavity field).

With the above example ($Q = 10^{10}$, $f = 1.3$ GHz) the decay time constant is 2.4 sec and can be measured easily. The drive power is switched by the p-i-n modulator in Fig. 5.

The accelerating voltage U now can be calculated with Eq. (3) and (6) because R/Q, Q and P are known. The on-time of the pulsed RF power has to be long enough for complete filling of the cavity.

$$U(t) = U \cdot (1 - e^{-\frac{t}{\tau}}) \tag{8}$$

where:

$U(t)$ is the time dependent filling of the cavity field,
t is the time since switching on the resonator
U is the value of the cavity field after complete filling.

Figure 6 shows the microwave signals of a measurement set up for superconducting cavities according to the arrangement of Fig. 5. In this example, the RF drive is switched on for 20 sec. The cavity voltage increases (Eq. (8)) and for 10 sec a flat top of U is reached. After switching off the generator, the cavity field decays (Eq. (6)) and the decay constant is measured to determine the quality factor.

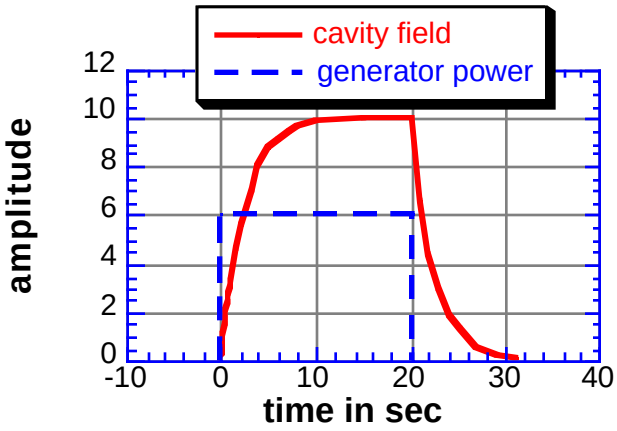

Fig. 6 Oscilloscope trace of the cavity voltage for a pulsed generator power. The example is given for the following parameters: f_0 = 1.3 GHz, Q_0 = 10^{10}, generator power is 70 W, 9-cell cavity with R/Q-value of 1000 Ω (TESLA case).

3. FIELD LIMITATION BY MULTIPACTING

The first superconducting cavities were made from lead (in the late sixties). Then niobium was chosen as material because of its superior properties (T_c = 9.25 K, B_c = 190 mT as compared to T_c = 7.2 K and H_c = 804 G for lead). Figure 7 shows a cross section of such an early Nb resonator. The two cups were machined from a solid Nb cylinder and welded at the equator. This fabrication technique as well as the shape (long cylindrical part at the equator, sharp corner at the transition to the iris) is typical for the design of normal conducting resonators. The cavity was measured in the pulse mode technique with the frequency stabilisation circuit as described before. The measurements, however, showed dramatic deviations as compared to the expected curve (see Fig. 8). The cavity started filling, but at a certain field value, no further increase could be gained. The excessive forward RF power was absorbed by the cavity without any increase of the field level. The transition at the limiting field was sharp. Sometimes a low level barrier could be overcome, but the same limiting phenomenon started at a somewhat higher field level again.

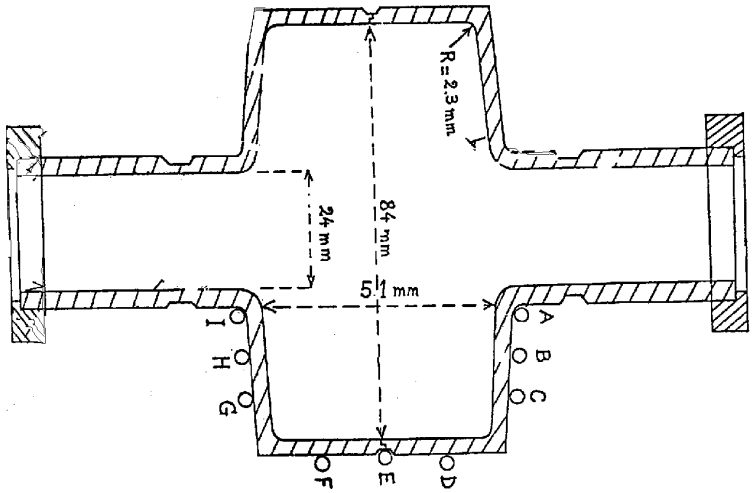

Fig. 7 Cross section of an early superconducting resonator. A cylindrical part at the large diameter and a sharp corner at the transition to the iris region is typical for this design.

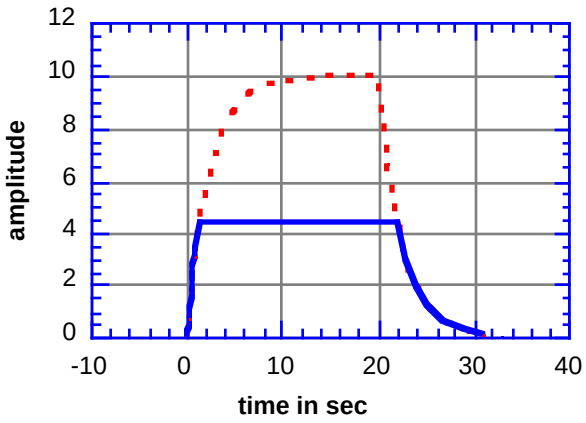

Fig. 8 Oscilloscope trace of the cavity field. The multipacting phenomenon (see text) limits the cavity field with a sharp transition at low field levels.

The analysis of the experimental observation concluded that at a certain field level all additional RF power was absorbed by an unknown mechanism. This kind of resonant absorption suggested that multiple electron impacting, so-called "multipacting" might be involved in the limiting mechanism. An electron avalanche is initiated by the multipacting effect at certain resonant conditions of the electromagnetic field. The multipacting current withdraws energy from the electromagnetic field. The magnitude of the multipacting current is stabilised to such a value that the cavity field is limited at the critical value.

A simple example of multipacting happens in the electric field between parallel plates (see Fig. 9). A first electron is accelerated by the electric field and crosses the gap to the other plate during one half RF cycle. If the time of flight is $N \cdot T/2$; $N = 1, 3, 5 \ldots$; T = period time; the electron could cross the gap backwards again (resonant conditions). If the impact energy is in the range between 50 eV and 500 eV (depending somewhat on the type of metal and surface condition), more than one primary electron will be created (see Fig. 10). Thus an electron avalanche will grow and absorb any RF power which exceeds the necessary value to establish the field value at the resonant condition.

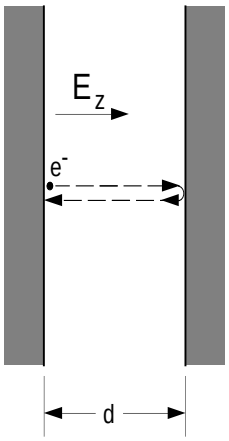

$$E_z = E_0 \sin(\omega t); \quad B=0$$

$$\omega t_n = (2n-1)\cdot\pi$$

$$m\,\ddot{z}(t) = q\,E_0 \sin(\omega t)$$

$$\Rightarrow E_n \propto \frac{d\,f^2}{2n-1}$$

Fig. 9 Parallel-plate geometry as example of two-side multipacting in a time dependent electric field

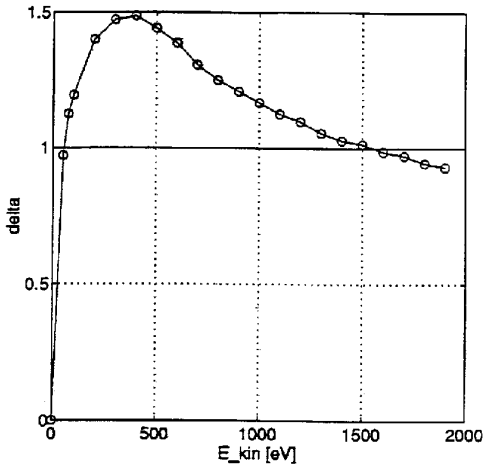

Fig. 10 Production rate (delta) of secondary electrons after impacting a metal surface by one primary electron (= secondary yield) as function of the impact energy

There was the suspicion that such a two-point multipacting between both end plates of the resonator might be the reason for the observed limitation. The counter argument is that the magnetic field component of the resonator field (azimutal field around the axis of rotation) will bend the electrons to the outer wall and prevent a closed orbit.

Experiments were undertaken to find the location of enhanced losses. Temperature sensors were placed at the outer cavity wall. The temperature sensors were specially selected carbon resistors with a high gradient of resistivity vs. temperature at the operating temperature between 4.1 K and 1.8 K. Heat pulses were detected at the outer cylindrical wall next to the iris transition. To simulate a possible multipacting resonance, tracking codes were developed. The trajectory of an electron which was started at the suspicious surface of the cavity area was calculated under the influence of the electromagnetic field. Resonant electron trajectories were found. Figure 11 gives an example of these trajectories. The characteristics of this multipacting are as follows:

- Electrons start and return to the same surface ("one-point multipacting").
- The resonant trajectories are closed orbits with the shape of a circle (first order, N=1) of an eight-like shape (second order, N=2), double-eight-like shape (third order, N=3) and so on.
- The closed orbit is created by the bending force of the magnetic field (cyclotron resonance). Only a small electric field is needed to accelerate the electron away from the surface.
- The trajectory circle is very small compared to the cavity dimensions (only about 1 % or less). Earlier simulations did not find these resonances since the cavity cross section was scanned with a mesh size in the dangerous area that was too large to resolve the trajectories.

The most successful remedy against this one-point multipacting was the design of a cavity shape which avoids the conditions for multipacting: no constant magnetic field along the surface and strong electric field to eject electrons far away from the dangerous surface. These conditions are fulfilled by a spherical (or more generally by an elliptical) cross section of the cavity [17]. Figure 12 shows such a favourable cavity shape. There is no cylindrical part with constant magnetic and low electric field. There is a zero crossing of the electric field at the

equator (from conditions of symmetry) and the field strength of the electric field increases strongly due to the fast transition to the iris geometry. It was observed that another type of multipacting is created at this geometry: two side trajectories crossing the equatorial plane. Fortunately these trajectories proved to be unstable so that in the experiment this limitation could be overcome easily.

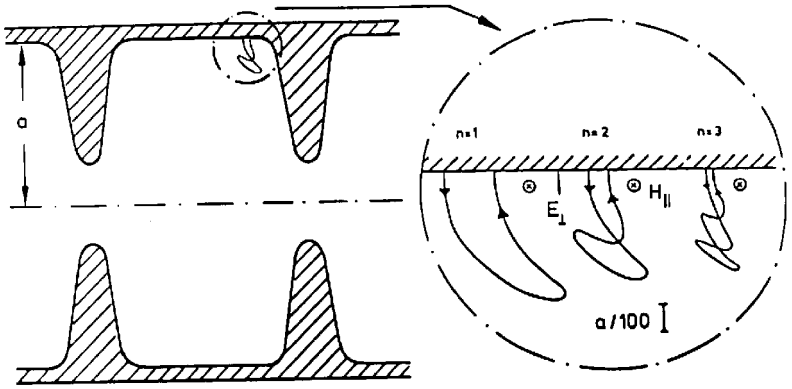

Fig. 11 Trajectories of "one-point" multipacting in resonators with a long cylindrical part at the large diameter

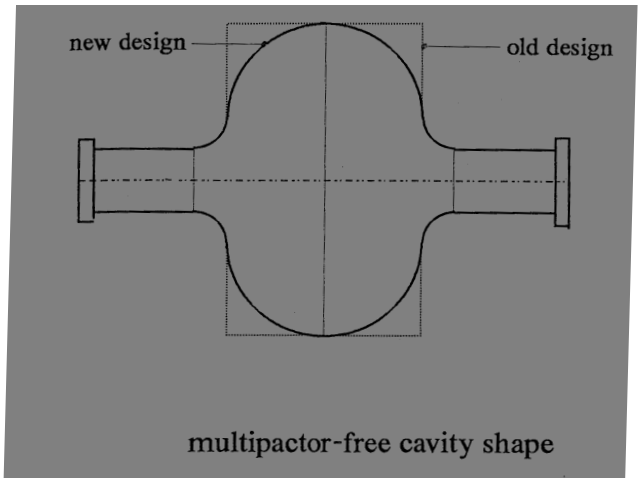

Fig. 12 New cavity shape to suppress multipacting. The spherical (or generally speaking the elliptical) cross section of the cavity avoids resonant conditions for multipacting. The "old" cavity shape with sharp corners and a cylindrical outer contour is shown in dashed lines. This shape produces multipacting resonances.

4. FIELD LIMITATION BY QUENCH

After the elimination of multipacting, higher gradients of superconducting cavities were expected. Figure 13 shows that a new type of limitation was observed. The cavity experienced a regular filling behaviour. At some level, however, the stored energy was absorbed during a time period much shorter than the natural filling time constant. The field in the cavity went to nearly zero (less than 1 % of the value just before the breakdown) and remained at this condition for some time although the generator offered forward power continuously. After some time the cavity started filling, reached the critical value and broke down again.

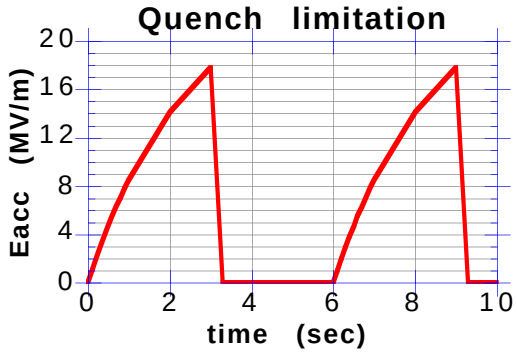

Fig. 13 Typical oscilloscope trace of the cavity field with a breakdown due to a quench

The diagnostic system to detect locations of enhanced losses in a cavity had been further developed. Instead of installing many fixed temperature sensors to the outer wall of the cavity (which means assembly effort to place the thermometers in good contact with the cavity surface and to dismantle all after the test), a system of rotating sensors has been developed. A frame with about 200 resistors per 1 metre cavity length is installed around the cavity. The temperature of the sensors and thus the temperature of the outer cavity wall is measured for the condition of high field and no field in the cavity at one angular position. Then the resistor frame is rotated (by about 3°) and a new measurement is carried out. In this way a temperature map of the whole cavity surface is created. This diagnostic tool gives valuable information about the location, spatial distribution and (if calibrated) about the absolute value of the dissipated power. Figure 14 gives an example of the mechanical arrangement, Fig. 15 shows a typical temperature map indicating the presence of one hot spot. After localising, the hot spot cavities were inspected from the inside to identify the reason of the breakdown. In many cases "defects" were detected: cracks in a weld, foreign particles sitting on the surface, "drying spots" from the last water rinsing etc. These findings concluded the following breakdown mechanism (see Fig. 16):

- A normal-conducting particle is sitting at the surface and produces enhanced RF losses.

- The enhanced heat is transferred through the niobium to the outside cooling helium. Therefore the temperature of the inner niobium surface next to the normal-conducting defect is raised.

- With increasing RF field, the heat production of the normal-conducting spot is increased and the surface temperature rises further.

- At a critical RF field the niobium surface next to the hot spot reaches the transition temperature of niobium (or strictly speaking: the reduced critical field at the enhanced temperature is reached).

- The niobium underneath the hot spot will switch to normal conductivity and further increase the heat flux. Finally the normal-conducting area will grow and dissipate the stored cavity energy in a short time. This breakdown process is named a "quench".

There are two principal ways to reduce the quench limitation:

1 Any kind of contamination has to be avoided by quality control of the niobium, extremely careful cleaning of the cavity surface and final handling of the cavity under best dust-free conditions. Also auxiliary equipment (pumping lines, coupler, etc.) has to be treated in the same way to avoid contaminating the cavity surface.

Scratches of the niobium or "loose" niobium particles (welding balls) have to be avoided, too.

2 If there are remaining defects on the surface, the other way is to improve the thermal conductivity of the niobium itself. In this way the temperature increase due to enhanced heat flux is reduced. Model calculations concluded [18] that the quench field (due to a normal-conducting spot) increases with the square root of the thermal conductivity of the niobium. This is valid as long as the Kapitza resistance (= thermal resistance of the Nb-to-liquid-helium interface) is small compared to the thermal resistance of the Nb itself.

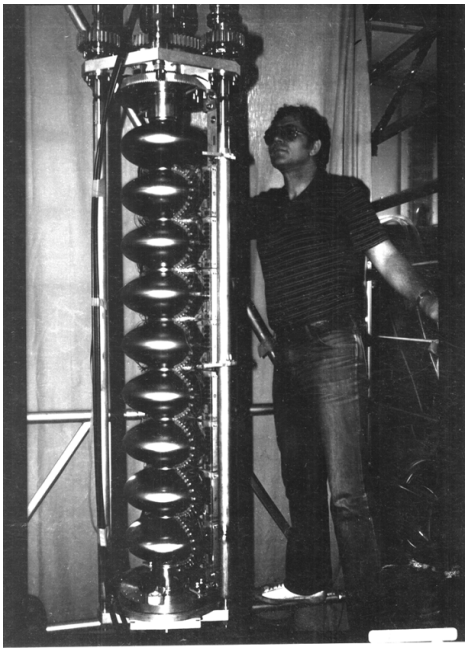

Fig. 14 A rotating temperature-mapping system assembled around a 9-cell 1.0-GHz niobium cavity. Carbon resistors are used to detect heat pulses from "bad spots" inside the cavity.

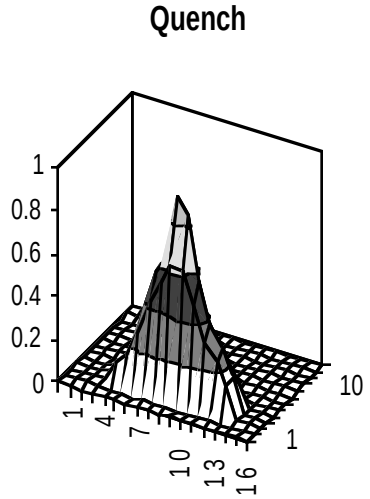

Fig. 15 Typical temperature map showing a single heat spot. In this plot the azimuthal and meridial position of the temperature sensor is transferred in rectangular x, y coordinates. The vertical amplitude corresponds to the measured increase of temperature.

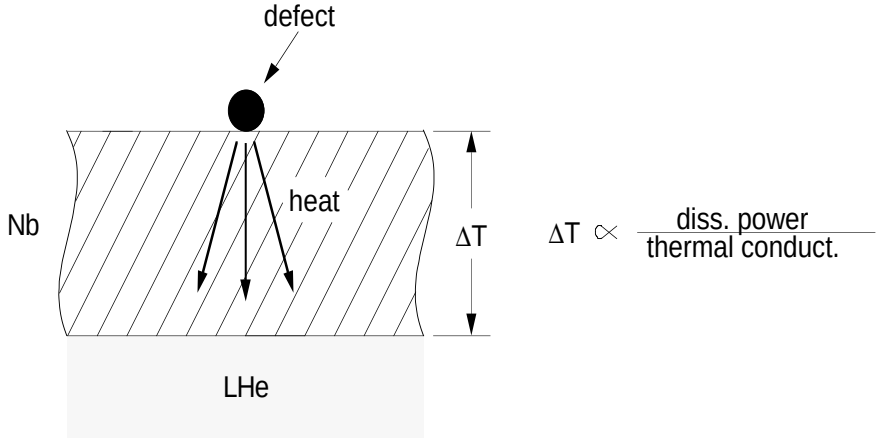

Fig. 16 Model of a breakdown due to excessive heating by a local defect ("quench").

Great progress has been made in clean treatment and improved thermal conductivity of the niobium during the last decade. Nevertheless, more effort is needed to transfer the excellent performances of single-cell cavities to real accelerating structures with all their auxiliary equipment (couplers, HOM dampers, tuners, etc.).

5. LIMITATION BY FIELD EMISSION OF ELECTRONS

If a cavity does not show multipacting or quench behaviour, a third type of phenomena usually limits the available gradient. Figure 17 demonstrates such a limitation. At first the cavity follows the expected filling curve. But at higher field levels, the rate of increase of the electric field slows down. An equilibrium level is reached which is lower than the expected value. If the generator power is raised further, the cavity field value is only slightly enlarged. This behaviour can be more clearly analysed if the standard Q vs. cavity voltage diagram is plotted (see Fig. 18). At low field values, the cavity quality factor stays constant (as expected). At high fields, the quality factor drops down dramatically for further increased cavity voltage. Under these conditions, γ-ray activity is noted outside the cryostat. A temperature map shows the locations of additional heat dissipation (see Fig. 19). Heat is produced along a line. If the temperature map is orientated like the projection of a globe (the beam axis penetrates the north and south pole) then the line of loss always follows a meridian.

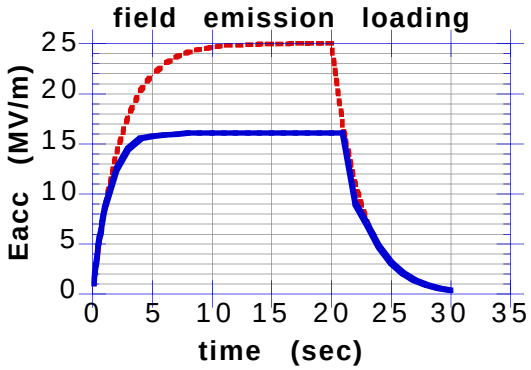

Fig. 17 Typical oscilloscope trace of the cavity field with field emission loading. The field follows the expected filling curve up to some critical value. Above this level the increase of the cavity field is considerably reduced and an equilibrium state is reached which is lower than the calculated value.

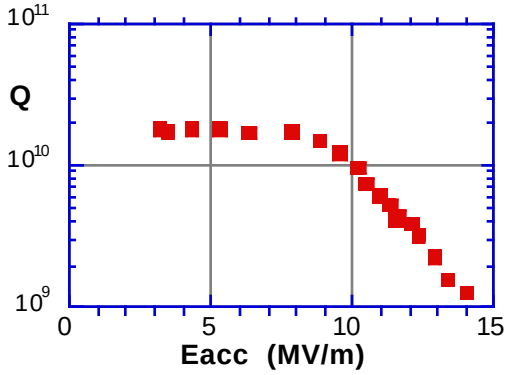

Fig. 18 Measured quality factor of a cavity versus accelerating gradient. Above 10 MV/m field, emitted current is present and is accelerated by the RF field. This results in additional losses so that the quality factor decreases.

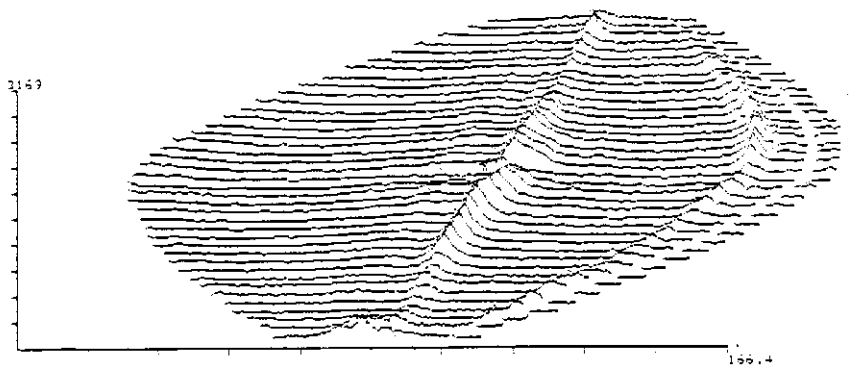

Fig. 19 Temperature map of a cavity loaded by field emission current. Two emitters produce two lines of additional losses. The lines follow a meridian.

The explanation of this limitation is that electrons are produced by field emission at the location of high surface electric fields, i.e. at the area of the iris. Then electrons are accelerated by the electric fields of the cavity. Because of the rotational symmetry of the cavity, there is no azimutal electric field compound (in the accelerating mode TM_{010}). Therefore the electron will hit the cavity surface along a meridian line and produce heat by impact.

Field emission of metal surfaces is a tunnel effect of electrons through the surface barrier. The extracted current grows exponentially (Fowler-Nordheim, see Bonin's chapter) with the surface field. That explains why the quality factor of the cavity rapidly decreases (i.e. the additional losses increase quickly) beyond the onset of field emission.

Field emission studies with DC and RF fields conclude that particles on the surface are the most likely reason for field emission. Here the microscopic electric field is enhanced by geometric effects. Although particles could be identified as the source of field emission, the detailed mechanism of why some emit but many do not is not understood. A detailed description of RF field emission is given in B. Bonin's chapter.

6. STATE OF THE ART

6.1 Results of large scale production

Niobium sheets for cavity production can be obtained from industry in high quality. A thermal conductivity values of 75 W/mK at 4.2 K is a standard quality. Usually the value of RRR (residual resistance ratio: ratio of electric resistance at room temperature and at 4.2 K in the normal-conducting state) is quoted because this quantity is easier to be measured. RRR and thermal conductivity values are related to each other (Wiedemann-Franz law) and the above value corresponds to RRR = 300. This is an improvement of a factor ten compared to the first cavities for storage ring application. Progress was made in handling, welding and dust free assembly of cavities, too.

At CEBAF, 338 Nb cavities (5-cell, 1.5-GHz) were fabricated during 1991–1994 by industry and chemically treated and assembled by the laboratory. The Nb sheet material has a RRR value of around 250. This is a large data base of cavity performance and is discussed here as a representative of the state of the art of superconducting cavity production. The cavities are assembled in pairs and are measured in a vertical cryostat. After this acceptance test, four pairs are grouped in a (horizontal) cryostat for installation in the accelerator tunnel. The vertical pair measurements gave the following results:

- Figure 20 shows the three typical qualities of performance: limitation by field emission (here at 10 MV/m) with the typical fast Q degradation by field emission; limitation by a quench with a nice flat Q vs. E_{acc} behaviour until quench break down at 13 MV/m; finally one of the best cavities which could be operated up to 19 MV/m (limited by available RF power)

- Figure 21 shows a "scatter plot" of the maximum gradient and Q values reached in all cavities during acceptance tests. It can be seen that the average value is 9.8 MV/m, but that there is a large spread of performance from 3 MV/m up to 18 MV/m.

- The cavities are limited by quench or field emission to about the same amount.

All cavities have been installed in the tunnel and commissioning of the linac started at the end of 1994. The design gradient is 5 MV/m. It will be interesting to see whether the cavity performance is preserved from vertical pair test to operation in the linac.

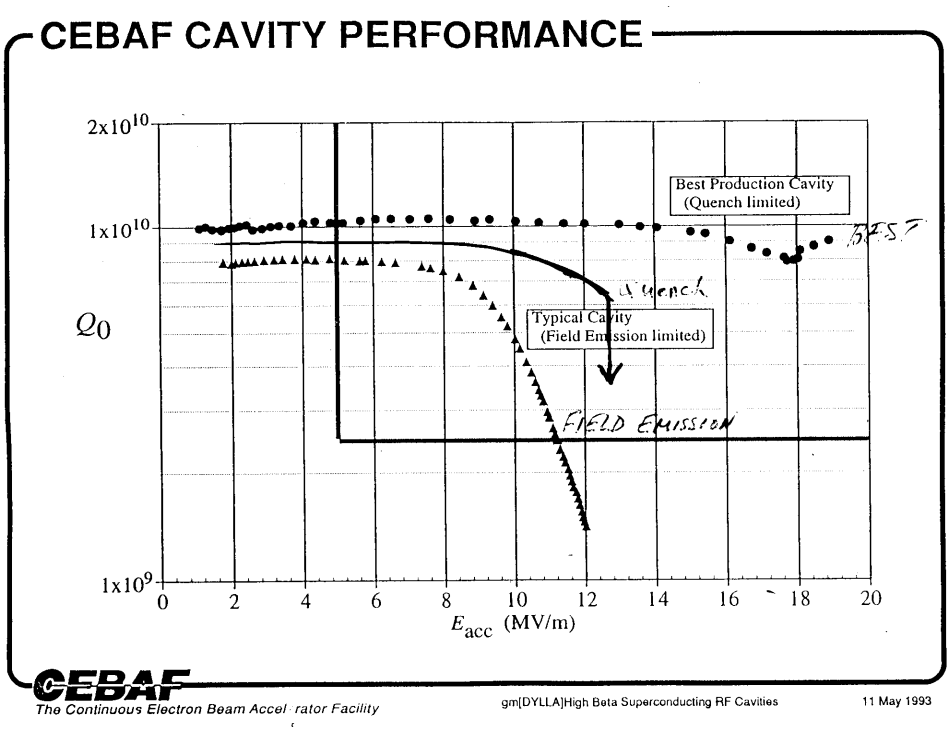

Fig. 20 Measurement of 5-cell (1.5-GHz) cavities at CEBAF. The three cavities are representatives of the typical performance: limitation by quench, field emission or (best cavity) only by available RF power.

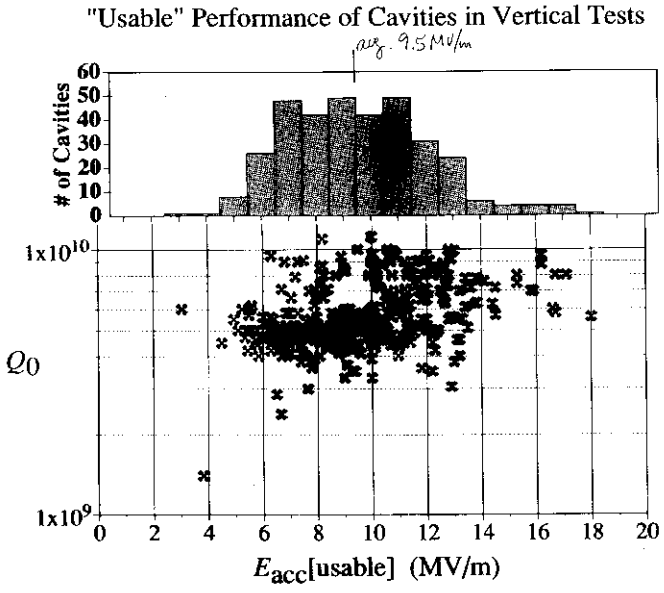

Fig. 21 Performance of all 338 CEBAF 5-cell cavities (1.5-GHz) during their acceptance test (pair measurement in vertical cryostats).

6.2 Automized chemistry and clean-room assembly

It has been mentioned that dust particles are the most likely source of field emission. Therefore absolutely clean conditions are essential to prepare a high-gradient cavity. The standard procedure of cavity fabrication is to make cups from niobium sheets (by deep drawing

or spinning) and to weld those cups at the equator and iris region by electron-beam welding. After fabrication the cavity surface is cleaned by removing about 100 μm of the niobium material at the inner surface. This is done by etching the niobium with a solution of H_3PO_4, HNO_3 and HF. Is is important to use the best grade of acid to avoid contamination of the clean niobium surface by residues in the acid. After the acid treatment the niobium surface has to be rinsed with high quality clean water. The best result can be expected if a closed circuit of acid treatment, water rinsing and subsequent drying is installed. Such a system has been developed at Saclay and is being used for the TESLA Test Facility (TTF) at DESY (TESLA = TeV range Electron Superconducting Linear Accelerator). After this treatment couplers, higher-order mode dampers, pick-up probes etc. have to be attached to the cavity. This must be done under dust-free conditions, too. Therefore clean rooms are installed at all laboratories which handle superconducting cavities. The quality of the clean room is class 10 (10 particles of μm size per cubic foot and minute) and corresponds to the requirements in semiconductor industry.

6.3 High-pressure water rinse

Sapphire samples have been used to measure the cleanliness of the standard niobium surface treatment. These samples accompanied the niobium during each step of treatment. Afterwards the size and number of particles on the surface were measured with a laser reflectometer. The result was that hundreds of particles (per square inch) of μm size are still present on the surface. Spraying the surface with high-pressure water (about 100 bar) is a common method in the semiconductor industry to further clean the surface. Recently the same method has been used to clean cavities. At the TTF (DESY) a 2-m long rod is inserted in the vertical cavity after chemical etching and rinsing is done with ultra-pure water. The head of the hollow rod has a spraying nozzle and is slowly rotated and moved along the cavity axis to reach the whole inner cavity surface for cleaning. This high-pressure water cleaning is now the standard cleaning procedure for the TTF cavities. Figure 22 shows the improvement of the cavity performance after such a high-pressure water rinse.

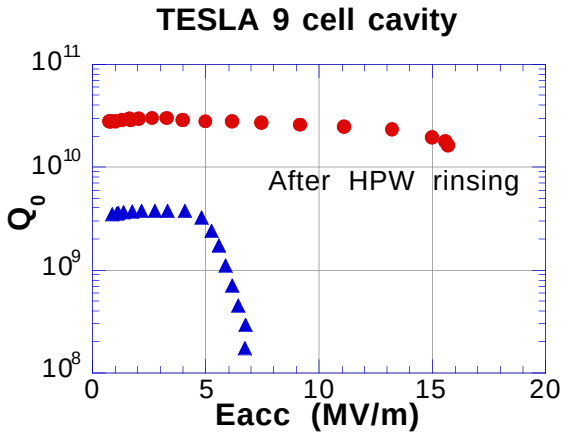

Fig. 22 Best improvement of cavity performance after high pressure water cleaning.

6.4 Post purification by Ti heat treatment

A high thermal conductivity of the niobium is essential to avoid limitation by quench. During welding of the niobium cavities using an electron-beam welding machine, the hot niobium can absorb oxygen, carbon or nitrogen due to insufficient vacuum conditions. This will result in a reduced thermal conductivity at the welded region. Unfortunately, the weld at the equator is at the location of highest surface current. Therefore a post purification of the niobium cavity after fabrication could "repair" the thermal conductivity at those deteriorated regions and improve the thermal conductivity elsewhere. The procedure is to heat the cavity

and some titanium (placed inside and outside the cavity) at 1400 °C for about 4 hours. The evaporated Ti covers the niobium surface. The Ti film will getter dissolved gases (O, C, N) from the bulk niobium because of its higher affinity compared to niobium. The mobility of the dissolved gases in niobium at 1400 °C is high enough to acheive a sufficient cleaning of the bulk niobium by this solid-state diffusion process within 4 hours. After the heat treatment the cavity has to be cleaned of Ti by etching away about 100 μm of Nb surface. Typically the thermal conductivity can be improved by a factor of 2–3 by this procedure. It has to be mentioned, however, that the niobium is softened by the heat treatment (the yield strength $\sigma_{0.2}$ reduces typically from 40 N/mm^2 to 10 N/mm^2). This reduced mechanical strength has to be compensated by careful handling and the use of appropriate fixtures during assembly of the cavities.

6.5 High power processing

Investigation of RF field emission leads to the conclusion that small particles are the origin of the emitted current. Therefore very careful cleaning is needed to suppress this limitation. Nevertheless, some "residual" dust will remain on the surface or may contaminate the cavity during the final assembly procedure. Therefore an "in situ" cleaning procedure, which can be applied after assembly or during operation of the superconducting cavity is of great help. Such a method was developed at Cornell recently [19] and has been successfully applied at several laboratories. The cavity is operated with short (approx. 50 to 500 μsec) RF pulses of high power (about 1 MW for a 9-cell TESLA cavity, 1.3 GHz). The cavity is heavily overcoupled to the feeding line in order to reduce the filling time (some 100 μsec, TESLA cavity) as compared to a matched superconducting resonator (about 1 sec, TESLA cavity). Therefore the cavity field reaches a high value in a short time. A field emitter will heat up, accordingly, and reach a high temperature. The process is a transient behaviour so that a thermal equilibrium state is not yet reached. Many photos of such an event suggest that the emitting particle is "exploded" due to excessive heating. Figure 23 shows such an exploded emitter and its characteristic "star burst" signature.

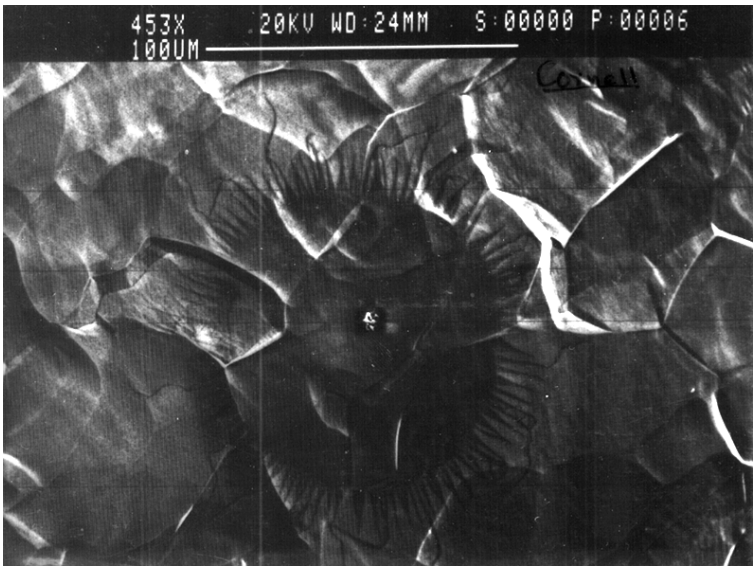

Fig. 23 "Star burst" picture of a field emitter after processing with high peak RF power. It is assumed that the field emitting particle "explodes" during the processing.

During high power processing, many processing events are observed by a short breakdown in the stored cavity field. Figure 24 shows a typical Q vs. E_{acc} curve before and after high power processing. It can be seen that the onset of field emission is considerably enlarged. There is a concern that the left over material of an exploded field emitter might raise the RF loss of the cavity or produce new field emitters. Indeed, it is observed that the Q of a

cavity is slightly reduced after high power processing. But this is the only known way to cure a cavity from field emission in situ, i.e. without dismantling, cleaning and repeated cool down.

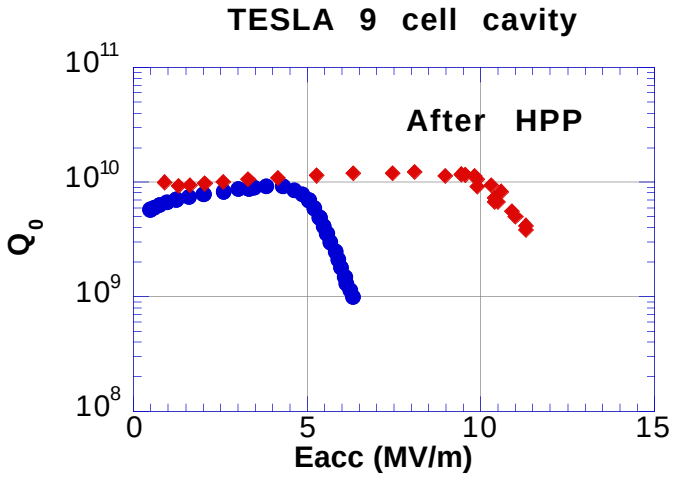

Fig. 24 Performance of a cavity before and after processing with high peak RF power

6.6 Best results of single and multicell cavities

It is a general finding that high gradients can be reached more easily with single-cell cavities than with multicell cavities. This is explained by a statistical model for the defect probability. In case of field emission this is justified by the observation that many small particles (i.e. possible field emitters) can still be found on a thoroughly cleaned surface. In the case of a quench defect, the statistical argument seems to be plausible, too. Therefore single-cell cavities are good test vehicles to investigate new treatment methods, or to search for the next high gradient limits. Considerable effort in quality control, cleaning and handling techniques is needed, however, to transfer the results from single cell cavities to multicell structures.

Single-cell activities at KEK [20] and CEBAF [21] are presented here as an example. At KEK niobium material with moderate thermal conductivity (RRR = 200) from Japanese companies is used. The cavities are electropolished by 200 μm. This gives smoother surfaces but the injected hydrogen (during the electropolish) must be removed by a moderate heat treatment at around 750 °C. Finally the cavities are slightly (20 μm) chemically etched and cleaned by high pressure water. Figure 25 shows that gradients around 30 MV/m with low field emission could be reached. All tests were finally limited by thermal quench.

At CEBAF [5], single-cell niobium cavities are post purified by the 1400 °C Ti treatment, followed by chemical etching (150 μm) and high-pressure water rinsing. The best measurement is shown in Fig. 26. The measured gradient of 43 MV/m comes close to the expected theoretical limit of 50 MV/m (with the corresponding surface magnetic field equal to the thermodynamic critical field). It should be noted that this high field was measured at the rather low temperature of 1.5 K. Many other tests with single cells reached gradients around 30 MV/m with only slight field emission.

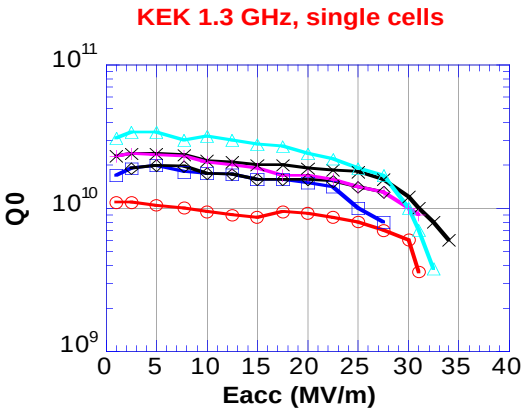

Fig. 25 Recent single-cell measurements (1.3 GHz) at KEK. All fields were limited by quenches.

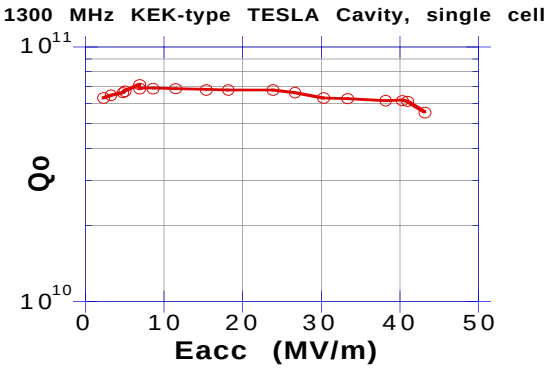

Fig. 26 Best single-cell measurements (1.5 GHz) at CEBAF (T = 1.5 K). The field was limited by quench.

At Cornell the technique of high power processing has been developed [19]. Several 5-cell cavities (TESLA shape; the furnace for the Ti treatment accepts no larger structures than 5 cells) have been processed. Figure 27 shows the improvement after high power processing. As a rule of thumb, the onset of field emission could be raised by a factor of 2.

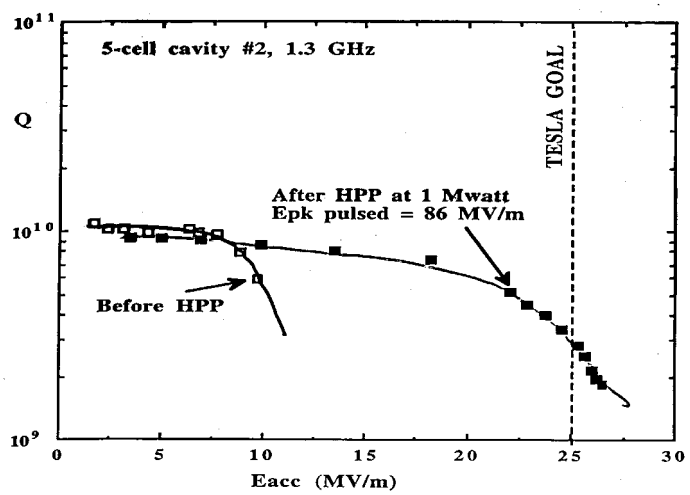

Fig. 27 Improvement of cavity performance by high power processing (HPP). Measurement of 5-cell, 1.3-GHz cavities at Cornell.

At DESY the infrastructure for processing of TESLA cavities was completed in 1994 and several 9-cell TESLA cavities (1.3 GHz) have already been measured. The standard procedure is:

- chemical etching of 100 µm to clean the niobium surface,
- Ti treatment at 1400 °C to improve the thermal conductivity,
- chemical etching of 100 µm to remove the Ti layer,
- high pressure water (100 bar) spray to clean the surface,
- high power processing to do in situ cleaning.

Figure 28 shows the measured Q vs. E_{acc} curve of the first series production cavity under continuous wave operation. The specified values for the test linac are Q = 3 x 10^9 at E_{acc} = 15 MV/m. In TESLA the superconducting cavities will be pulsed with 800 µsec flat top at 25 MV/m, rep. rate 10 Hz. These conditions could be established with the first series production cavity attached to a high power input coupler (see Fig. 29).

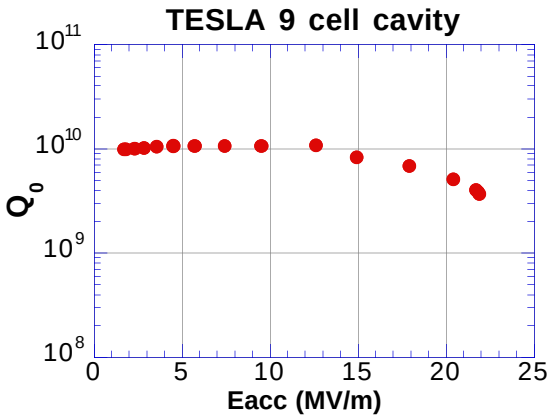

Fig. 28 Measurement of the first 9-cell TESLA cavity (1.3 GHz) under continuous wave operation

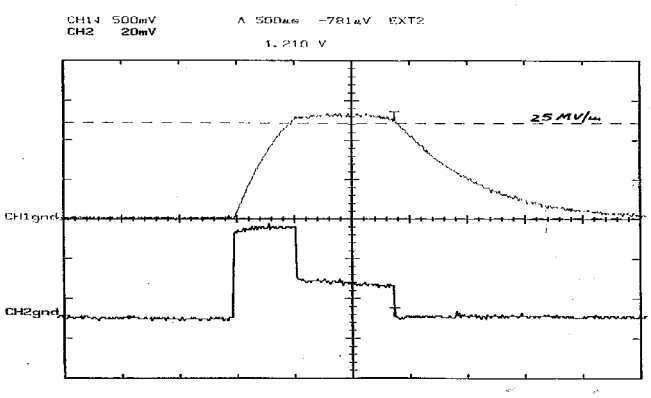

Fig. 29 Pulsed measurement of the first 9-cell TESLA cavity. The beam loading during the 800 µsec flat top was simulated by shaping the klystron power (upper curve E_{acc}, lower curve klystron power).

ACKNOWLEDGEMENTS

Exchange of information and stimulating discussions with my colleagues from CEBAF, CERN, DESY, Cornell, KEK and Saclay are gratefully acknowledged.

REFERENCES

[1] G. Cavallari et al, Acceptance Tests of Superconducting Cavities and Modules for LEP from Industry, Proc. EPAC 3, London (1994), p. 2042 - 2044.

[2] B. Dwersteg et al, Operating Experience with Superconducting Cavities in HERA, Proc. EPAC 3, London (1994), p. 2039 - 2041.

[3] S. Noguchi et al, Recent Status of the TRISTAN Superconducting RF System, Proc. EPAC 3, London (1994), p. 1891 - 1893.

[4] M. Castellano et al, Early Results of Beam Acceleration in the SC Linac LISA, Proc. EPAC 1, London (1994), pp. 731.

[5] A. Hutton for the CEBAF Commissioning Team, Commissioning at CEBAF, Proc. EPAC 1, London (1994), p. 15 - 19.

[6] M. S. McAshen et al., Appl. Phys. Lett. 22 (1973) 605 and J.R. Calarco et al, IEEE Trans. Nucl. Sci. NS-24 (1977) 346.

[7] S. Döbert et al., Status of the S-DALINAC and Experimental Developments, Proc. EPAC 1, London (1994), 719 - 721.

[8] R.C. Pardo et al, Operational Status of the Uranium Beam Upgrade of the ATLAS Accelerator, Proc. PAC 93, 3, (1993) p.1694 - 1699.

[9] G. Fortuna et al., Nucl. Instr. Methods A328 (1993) 236 and L. Badan et al, Contribution to the EPAC, London (1994).

[10] T. Ishii, M. Shibata, S. Takeuchi, Nucl. Instr. Methods A328 (1993) 231.

[11] H. Padamsee et al, Development and Tests of a Superconducting Cavity for High Current Electron Storage Rings, Proc. EPAC 3, London (1994), p. 2048 - 2051.

[12] T. Takashaki et al, 9th Symposium on Accelerator Science and Technology, Tsukuba, Japan, (1993) pp 327.

[13] M. Leenen for the TESLA Collaboration, The Infrastructure for the TESLA Test Facility (TTF) - A Status Report, Proc. EPAC 3, London (1994), p. 2060 - 2062.

[14] S. Ramo, J.R. Whinnery, T. van Duzer, Fields and Waves in Communication Electronics, Wiley Internat. Edition (1965).

[15] U. Laustroer, U. van Rienen, T. Weiland, URMEL and URMEL-T User Guide, DESY M-87-03 (1987) and T. Weiland, TBCI and URMEL - New Computer Codes for Wake Field and Cavity Mode Calculations, IEEE Trans. on Nuclear Science, vol NS 30 (1983) p. 2489 - 2491.

[16] M. Bartsch et al, "MAFIA Release 3. The New Version of the General Purpose Electromagnetic Design code Family," Proc. of EPAC Conf., Vol 1, pp 249-25 (1990).

[17] U. Klein, D. Proch, Proc. Conf. of Future Possibilities for Electron Accel., ed. JS McCarthy, RR Whitney. Charlottesville: Univ. Virginia (1979) p. N1-17.

[18] H. Padamsee, IEEE Trans. Mag. 19, (1983) 1322.

[19] C. Crawford et al, Achieving the TESLA Gradient of 25 MV/m in Multicell Structures at 1.3 GHz, Proc. EPAC 1, London (1994), p. 37 - 39.

[20] S. Noguchi, private communication.

[21] P. Kneisel, private communication.